Rectangular dielectric rod at microwave frequencies—Part I. Theoretical and experimental determination of launching efficiency

T. K. SEN* AND R. CHATTERJEE
Department of Electrical Communication Engineering, Indian Institute of Science, Bangalore 560012

Received on December 24, 1977

Abstract

The launching efficiency of surface-waves on a rectangular dielectric rod excited by a rectangular metal waveguide is derived theoretically. Experimental results for launching efficiencies obtained from the measurements of the scattering parameters of the junction between the launcher and the dielectric rods following Deschamp's method are compared with the theoretical results.

Key words: Dielectic rod, microwave frequencies, launching efficiency

1. Introduction

Theoretical determination of launching efficiency involves the solution of source excited fields. The results available at present on the excitation of surface-waves on various structures are mostly restricted to delta-function sources. A critical survey of the existing methods is given in the literature[1,2]. The case of finite aperture as source is difficult to solve theoretically. Rigorous solutions based on Wiener-Hopf techniques have been applied only to the case of structures which can be specified as reactance surfaces[1,3]. Unfortunately the above method is rather difficult to apply to a rectangular dielectric rod for which the surface reactance is a function of position on the surface.

In this paper, a simpler method is adopted for the case of aperture excitation. From the unperturbed fields tangential to the feed aperture planes the angular spectrum[4] of the aperture is derived. The effect of placing the rectangular dielectric rod in front of the aperture is to convert a portion of the angular spectrum confined within a cone whose axis coincides with the axis of the rod and whose semivertical angle is θ_e, where θ_e is the critical angle depending on the dielectric constant of the material of the rod. The remaining portion of the angular spectrum between θ_e and $\pi/2$ is radiated into free-space[5]. The power in the surface-wave modes and in the radiation field can be calculated separately because they are orthogonal. The launching efficiency is defined as the ratio of the surface-wave power to the total power crossing the feed aperture. An experimental technique following Deschamp's method verifies the theoretical results.

* Presently in the Dept. of Physics, Delhi University, Delhi.

2. Theory

Angular spectrum of the feed-aperture fields

The feed system used for launching surface-waves on a rectangular dielectric rod is a rectangular metal waveguide of cross-sectional dimensions $a_2 \times b_2$ (Fig. 1) excited in the dominant TE_{10} mode.

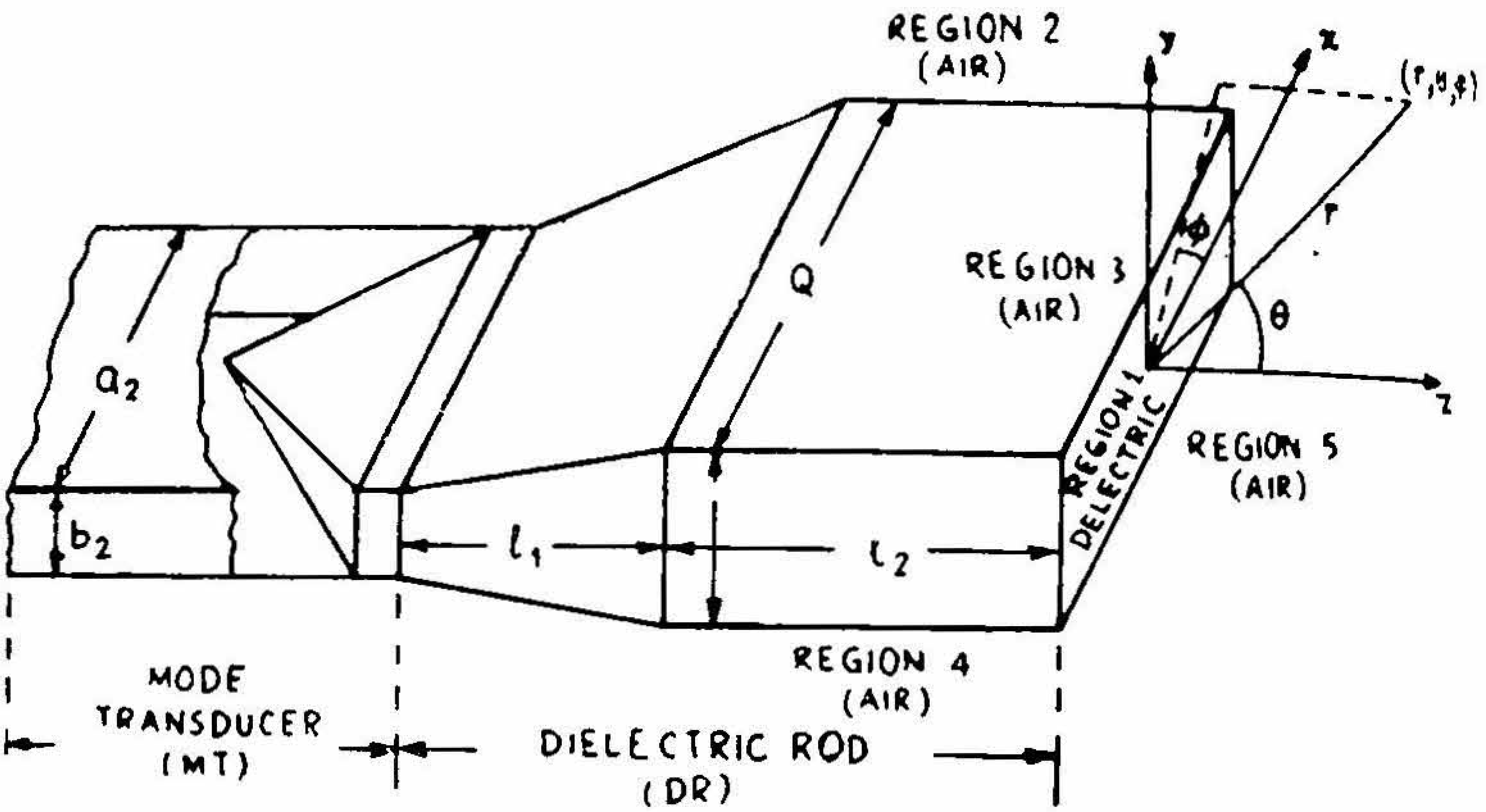

FIG. 1. Geometry of the mode transducer and the dielectric rod, MT = Mode transducer, DR = Dielectric rod.

The electric and the magnetic fields in the aperture ($Z = 0$) of the rectangular metal waveguide are given by

$$E_y = -\frac{\omega\mu_0}{\beta}\cos(\pi x/a_2) \tag{1}$$

$$H_x = \cos(\pi x/a_2).$$

If the spectral representation of H_x at this aperture $z = 0$ is given by,

$$F_M(k_x, k_y) = \int_{-\infty}^{\infty}\int H_x \exp j(k_x x + k_y y)\, dx\, dy \tag{2}$$

then the field at any point in an unbounded dielectric medium ($Z > 0$) is obtained as

$$H_x(x, y, z) = \frac{1}{4\pi^2}\int_{-\infty}^{\infty}\int T_M(k_x, k_y) \exp -j(k_x x + k_y y + k_z z)\, dk_x, dk_y \tag{3}$$

where (4)

$$k_x^2 + k_y^2 + k_z^2 = k_1^2 = \omega^2 \mu_0 \varepsilon_0 \varepsilon_r$$

and the relationship between $F_M(k_x, k_y)$ and $T_M(k_x, k_y)$ is to be found. The other field components are derived from Maxwell's equations as follows:

$$E_x = -\frac{1}{\omega\varepsilon_0\varepsilon_r k_z}\frac{\partial^2 H_z}{\partial x\,\partial y}$$

$$E_y = -\frac{k_x^2 + k_z^2}{\omega\varepsilon_0\varepsilon_r k_z} H_z$$

$$E_z = \frac{j}{\omega\varepsilon_0\varepsilon_r}\frac{\partial H_z}{\partial y} \tag{5}$$

$$H_y = 0$$

$$H_z = -\frac{j}{k_z}\frac{\partial H_x}{\partial x}\,.$$

If R_m is the reflection coefficient at the metal waveguide aperture ($z = 0$) the spectra components of E_y and H_x at $Z = 0$ are given by

$$E_y = -\frac{\omega\mu_0}{4\pi^2\beta}(1 + R_m) F_M \exp - j(k_x x + k_y y) \tag{6}$$

$$H_x = \frac{(1 - R_m)}{4\pi^2} F_M \exp - j(k_x x + k_y y) \tag{7}$$

At $z = 0+$,

$$H_x = \frac{T_M}{4\pi^2}\exp - j(k_x x + k_y y) \tag{8}$$

From equations (4) and (5)

$$E_y = -\frac{k_1^2 - k_y^2}{\omega\varepsilon_0\varepsilon_r k_z}\frac{T_M}{4\pi^2}\exp - j(k_x x + k_y y) \tag{9}$$

From the conditions of continuity of E_y, and H_x at $Z = 0$ we obtain

$$\frac{1 - R_m}{1 + R_m} = \frac{k_1^2 k_z}{\beta(k_1^2 - k_y^2)}$$

or

$$R_m = [\beta(k_1^2 - k_y^2) - k_1{}^2 k_z][\beta(k_1^2 - k_y^2) + k_1{}^2 k_z]^{-1} \tag{10}$$

and

$$T_M(k_x, k_y) = (1 - R_m) F_M(k_x, k_y). \tag{11}$$

Inserting H_x from equation (1) in equation (2) we obtain

$$F_M(k_x, k_y) = \frac{4\pi}{a_2}\frac{\cos(k_x a_2/2)}{(\pi/a_2)^2 - k_x^2}\frac{\sin(k_y b_2/2)}{k_y}\,. \tag{12}$$

(ii) *Effect of the finite dielectric medium*

The field represented by equation (3) is the field which will be present in an unbounded dielectric medium terminating the metal waveguide aperture. If the dielectric medium is finite in both the x and y directions (*i.e.*, in the present situation, a rectangular rod) a component plane wave will be multiply reflected by all the four sides of the rod. If R_x and R_y are the reflection coefficients of the yz and xz planes respectively, the resultant field due to an infinite number of reflections from the sides of the rod is given by

$$H_x = \frac{1}{4\pi^2} \int\int_{-\infty}^{\infty} T_M(k_x, k_y) \exp(-jk_z z) [\exp(-jk_x x) + R_x \exp(jk_x x)] [\exp(-jk_y y) + R_y (jk_y y)] . \times [(1 - R_x^2) (1 - R_y^2)]^{-1} dk_x\, dk_y. \tag{13}$$

From the continuity of B_x $(= \mu H_x)$ and D_x $(= \varepsilon E_x)$ at $x = \frac{a}{2}$ and E_x and H_x at $y = \frac{b}{2}$ respectively R_x and R_y are obtained as follows:

$$R_x = (k_x - p)(k_x + p)^{-1} \exp - j(k_x a) \tag{14}$$

$$R_y = (k_y - \varepsilon_r q)(k_y + \varepsilon_r q)^{-1} \exp - j(k_y b) \tag{15}$$

where

$$p = \pm [k_x^2 - (k_1^2 - k_0^2)]^{1/2} \tag{16}$$

$$q = \pm [k_y^2 - (k_1^2 - k_0^2)]^{1/2}. \tag{17}$$

The fields in the regions 2 and 3 (Fig. 1) are respectively given by

$$H_{x2} = \frac{1}{4\pi^2} \int\int_{-\infty}^{\infty} T_M(k_x, k_y)(D_x D_y)^{-1} \exp\left[j(p - k_x)\frac{a}{2}\right](1 + \rho x) . [\exp(-jk_y y) + R_y \exp(jk_y y)] . \times \exp[-j(px + k_z z)]\, dk_x\, dk_y \tag{18}$$

$$H_{x3} = \frac{1}{4\pi^2} \int\int_{-\infty}^{\infty} T_M(k_x, k_y)(D_x D_y)^{-1} \exp\left[j(q - k_y)\frac{b}{2}\right](1 + \rho_y). \times [\exp(-jk_x x) + R_x \exp(jk_x x)] \times \exp[-j(qy + k_z z)]\, dk_x\, dk_y \tag{19}$$

where

$$D_x = 1 - R_x^2 \tag{20}$$

$$D_y = 1 - R_y^2 \tag{21}$$

$$\rho_x = R_x \exp(jk_x a) \tag{22}$$

$$\rho_y = R_y \exp(jk_y b). \tag{23}$$

In the regions $x > \frac{a}{2}$ and $y > \frac{b}{2}$ the positive branches of p and q are taken to represent outgoing waves. k_x and k_y are in general complex and the integrals in equations (18) and (19) are to be evaluated in the complex plane.

(iii) *Evaluation of the ntegrals*

The singularities in the integrands of equations (18) and (19) are the surface-wave poles which are determined by $D_x = 0$ and $D_y = 0$. Dealing with even function modes these are equivalent to

$$R_x = 1 \tag{24}$$

and

$$R_y = 1 \tag{25}$$

For surface-waves the fields in the regions 2 and 3 should decay exponentially as $\exp(-\alpha_x x)$ and $\exp(-\alpha_y y)$ respectively. From equations (14), (15), (24) and (25) with $p = -j\alpha_x$ and $q = -j\alpha_y$ we obtain

$$\alpha_x = k_x \tan(\alpha_x a/2) \tag{26}$$

$$\varepsilon_r \alpha_y = k_y \tan(k_y b/2) \tag{27}$$

where from equations (16) and (17) we obtain

$$\alpha_x = [(k_1^2 - k_0^2) - k_x^2]^{1/2} \tag{28}$$

$$\alpha_y = [(k_1^2 - k_0^2) - k_y^2]^{1/2} \tag{29}$$

Only positive roots of α_x and α_y are considered to ensure that the surface-wave should decay away from the surfaces at $|x| = \frac{a}{2}$ and $|y| = \frac{b}{2}$ respectively. Equations (26) to (29) determine the transverse propagation constants of the allowed surface-wave modes of the dielectric rod.

Writing H_{z2} from equation (18) as

$$H_{z2} = \int_{-\infty}^{\infty}\int U(k_x, k_y)(D_x D_y)^{-1} dk_x dk_y \tag{30}$$

where

$$U(k_x, k_y) = \frac{T_M(k_x, k_y)}{4\pi^2} \exp\left[j(p - k_x)\frac{a}{2}\right](1 + \rho_x)$$
$$\times [\exp(-jk_y y) + R_y \exp(jk_y y)] \exp[-j(px + k_z z)] \tag{31}$$

the double integral for H_{z2} can be evaluated by the successive evaluation of two contour integrals[7] as follows:

$$H_{z2} = \int_{l_1} \int_{l_2} U(k_x, k_y)(D_x D_y)^{-1} dk_x\, dk_y \tag{32}$$

where l_1 and l_2 are two contours lying in the domains B_1 and B_2 where B_1 and B_2 are the domains of k_x and k_y respectively. $U(k_x, k_y)$ is regular in the closed domains B_1 and B_2. One contour is shown in Fig. 2. Applying Cauchy's residue theorem repeatedly we obtain

$$H_{z2} = -4\pi^2 \Sigma\, \Sigma\, U(\beta_x, \beta_y)(D'_x D'_y)^{-1} - 2\pi j\,. \\ .\, \Sigma \int_{\Gamma_1} U(k_x, k_y)(D'_y)^{-1} dk_x - 2\pi j\, \Sigma \int_{\Gamma_2} U(\beta_x, k_y)\,. \\ .\,(D'_x)^{-1} dk_y + \int_{\Gamma_1}\int_{\Gamma_2} U(k_x, k_y)(D_x D_y)^{-1} dk_x\, dk_y. \tag{33}$$

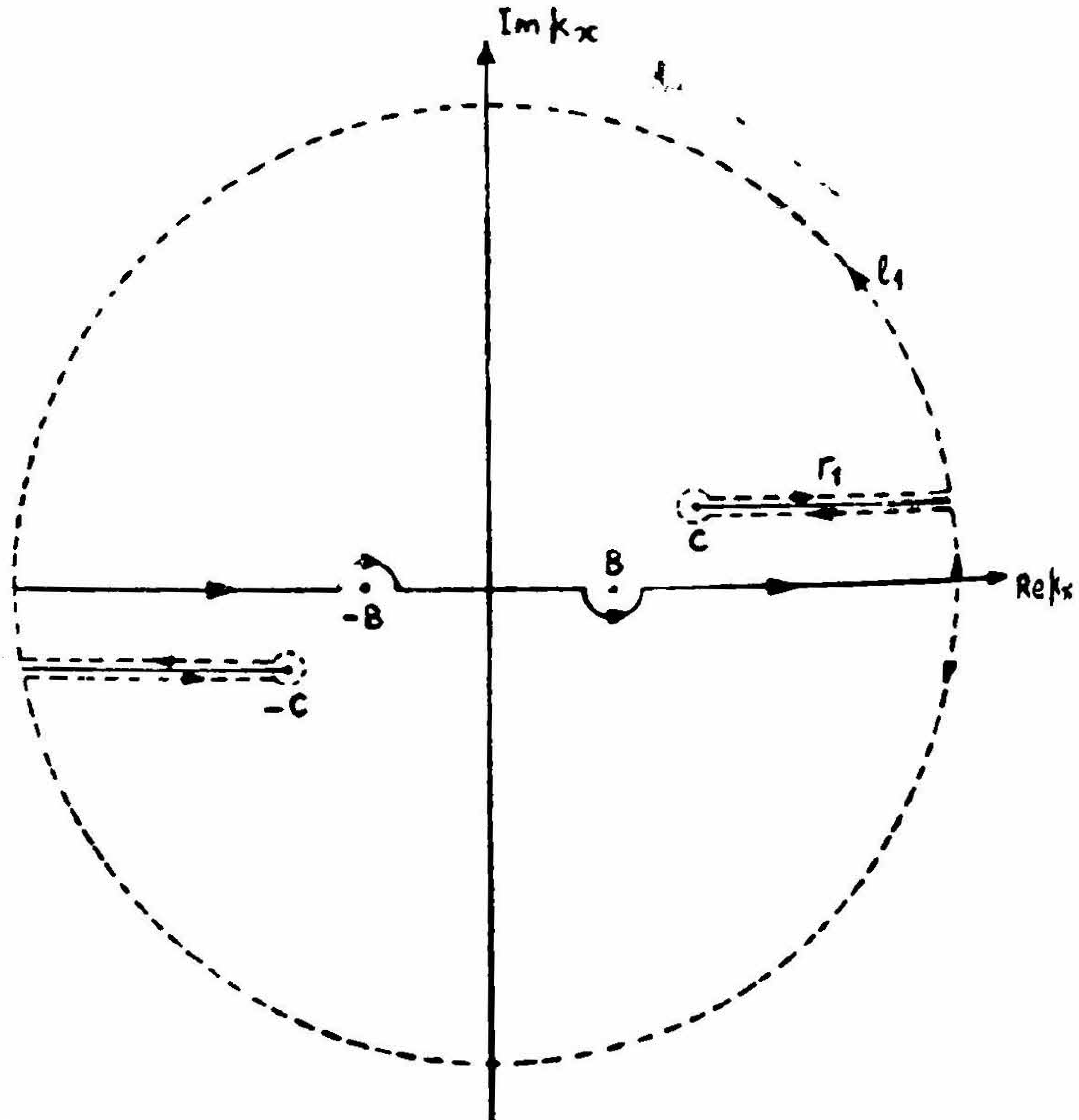

FIG. 2. Contour of integration.
Contour above Re (k_x) is for $x > 0$, contour below Re (k_x) is for $x < 0$

The summation is for all values of β_x and β_y where β_x and β_y are the roots of the transcendental equations (26) and (27) respectively and

$$D'_x = \left.\frac{\partial D_x}{\partial k_x}\right|_{k_x=\beta_x}$$

$$D'_y = \left.\frac{\partial D_y}{\partial k_y}\right|_{k_y=\beta_y}$$

Using equations (14), (15), (20) and (21) with $p = -j\alpha_x$ and $q = -j\alpha_y$ we obtain

$$D'_x = 2j\,(a + 2\alpha_x^{-1}) \tag{34}$$

and

$$D'_y = 2j\,[b + 2\varepsilon_r\,(\beta_y^2 + \alpha_y^2)\,\{\alpha_y\,(\beta_y^2 + \varepsilon_r^2\,\alpha_y^2)\}^{-1}]. \tag{35}$$

Inserting $U(k_x, k_y)$ from equation (31) in equation (33) we write

$$\begin{aligned} H_{z2} = &-4 \sum_{\beta_x} \sum_{\beta_y} T_M(\beta_x, \beta_y)\,(D'_x\,D'_y)^{-1}\cos(\beta_x\,a/2)\cos(\beta_y y).\\ &.\exp[\alpha_x\,(a/2 - x) - j\beta_x z] - \frac{4\pi j}{4\pi^2}\sum_{\beta_y}\cos(\beta_y\,y)\,(D'_y)^{-1}\,.\\ &.\int_{\Gamma_1} T_M(k_x, \beta_y)\,(D_x)^{-1}\,(1+\rho_x)\exp j\left[(p-k_x)\frac{a}{2} - px - k_z z\right]\\ &dk_x - \frac{4\pi j}{4\pi^2}\sum_{\beta_x}\cos(\beta_x\,a/2)\,(D'_x)^{-1}\exp\left(\frac{a}{2} - x\right).\\ &.\int_{\Gamma_2} T_M(\beta_x, k_y)\,(D_y)^{-1}\,[\exp(-jk_y\,y) + R_y\exp(jk_y\,y)]\,.\\ &.\exp(-jk_z\,z)\,dk_y + \frac{1}{4\pi^2}\int_{\Gamma_1}\int_{\Gamma_2} T_M(k_x, k_y)\,.\,(D_x\,D_y)^{-1}\\ &.(1+\rho_x)\,[\exp(-jk_y\,y) + R_y\exp(jk_y\,y)]\,.\\ &.\exp[-j\,(px + k_z\,z)]\,dk_x\,dk_y. \end{aligned} \tag{36}$$

Integrals around Γ_1 and Γ_2 are branch-cut integrals around branch points (C and $-C$ namely) $k_x = \pm\,(k_1^2 - k_0^2)^{1/2}$ and $k_z = (k_1^2 - k_0^2)^{1/2}$. Asymptotic evaluation of these integrals represents the far-field of the junction radiation. The second and the third integrals in equation (36) exert their influence in the far-field *via* the aperture $\left(|x| > \frac{a}{2}, -\frac{b}{2}, < y < \frac{b}{2}, Z = 0\right)$ illumination.

(iv) *Evaluation of branch-cut integrals*

We consider the first integral of equation (36) and denote it by I. Hence

$$I = -\frac{4\pi j}{4\pi^2} \sum_{\beta_y} \cos(\beta_y y)(D'_y)^{-1} \int_{\Gamma_1} T_M(k_z, \beta_y)(D_z)^{-1} \cdot$$

$$\exp\left[j(p - k_z)\frac{a}{2}\right](1 + \rho_z)\exp[-j(px + k_z z)]\,dk_z.$$

Let

$$F_z(k_y) = -\frac{4\pi j}{4\pi^2 D'_y} \int_{\Gamma_1} T_M(k_z, \beta_y) D_z^{-1} \exp\left[j p (p - k_z)\frac{a}{2}\right] \cdot$$

$$\cdot (1 + \rho_z)\exp(-jpx) \int_{-b/2}^{b/2} \cos(\beta_y y)\exp(jk_y y)\,dy.$$

(Using the spectral form and assuming that the fields in the region $|y| > \frac{b}{2}$ are very small). Evaluating the integral we obtain

$$F_z(k_y) = -\frac{4\pi j}{4\pi^2 D'_y}\left[\frac{\sin(Rb/2)}{R} + \frac{\sin(sb/2)}{S}\right] \int_{\Gamma_1} T_M(k_z, \beta_y)$$

$$\times (D_z)^{-1}(1 + \rho_z)\exp j\left[(p - k_z)\frac{a}{2} - px\right] dk_z \quad (37)$$

where

$$R = \beta_y + k_y$$

$$S = \beta_y - k_y \quad (38)$$

Then

$$I = \frac{1}{2\pi}\int_{-\infty}^{\infty} F_z(k_y)\exp[-j(k_y y + k_z z)]\,dk_y$$

$$= -\frac{2j}{4\pi^2 D'_y}\int_{-\infty}^{\infty}\int_{\Gamma_1} T_M(k_z, \beta_y)\left[\frac{\sin(Rb/2)}{R} + \frac{\sin(Sb/2)}{S}\right] \cdot$$

$$\cdot (1 + \rho_z)(D_z)^{-1}\exp j\left[(p - k_z)\frac{a}{2} - px - k_y y - k_z z\right] dk_z\,dk_y. \quad (39)$$

Evaluating the integral by stationary phase method (See Appendix) we obtain

$$I = -\frac{2\pi k_{z0}}{4\pi^2 r}\frac{2j}{D'_y D_z} T_M(k_z, \beta_y)(1 + \rho_z)\frac{p}{k_z}$$

$$\times\left[\frac{\sin(Rb/2)}{R} + \frac{\sin(Sb/2)}{S}\right]\exp j\left[(p - k_z)\frac{a}{2} - k_0 r\right]. \quad (40)$$

In a similar manner all the branch-cut integrals are evaluated. The total far-field in region (2) as given by equation (36) is

$$H_{z2} = \frac{2\pi k_{z0}}{4\pi^2 r}\Big\{ -2j\,\Sigma\,\frac{T_M(k_z, \beta_y)}{D'_y\, D_z} - \exp\,[j(p-k_z)\,a/2]\,(1+\rho_z)\,.$$

$$\times \frac{p}{k_z} T_M(k_z, \beta_y)\left[\frac{\sin(Rb/2)}{R} + \frac{\sin(Sb/2)}{S}\right] - 2j\,\Sigma\,\frac{T_M(\beta_z, k_y)}{D'_z\, D_y}$$

$$\times \cos(\beta_z a/2)\left[\frac{\exp(jpa/2)}{\alpha_z - jp} + \frac{\exp(-jpa/2)}{\alpha_z + jp}\right]$$

$$+ \frac{\exp(j(p-k_z)\,a/2)}{D_z\, D_y}(1+\rho_z)\frac{p}{k_z} T_M(k_z, k_y)\Big\}\exp(-jk_0 r) \qquad (41)$$

Proceeding similarly with the equation (19) and evaluating the branch-cut integrals the far-field in region (3) is given by

$$H_{z3} = \frac{2\pi k_{z0}}{4\pi^2 r}\Big\{ -2j\,\Sigma\,\frac{T_M(k_z, \beta_y)}{D_z\, D'_y} - .\left[\frac{\exp(jqb/2)}{\alpha_y - jq} + \frac{\exp(-jqb/2)}{\alpha_y + jq}\right]$$

$$-2j\,\Sigma\,\frac{T_M(\beta_z, k_y)}{D'_z\, D_y}\frac{q}{k_y}\,.\,\exp\,[j(q-k_y)\,b/2]\,(1+\rho_y)\,.$$

$$\times\left[\frac{\sin(pa/2)}{P} + \frac{\sin(Qa/2)}{Q}\right]$$

$$+ \frac{\exp\,[j(q-k_y)\,b/2]}{D_z\, D_y}(1+\rho_y)\frac{q}{k_y} T_M(k_z, k_y)\Big\}\,.$$

$$\exp(-jk_0 r) \qquad (42)$$

where

$$P = \beta_z + k_z \qquad (43)$$

$$Q = \beta_z - k_z. \qquad (44)$$

(v) ***Lanuching efficiency***

To determine the launching efficiency the total power carried by the surface wave and the power radiated from the junction are to be calculated. To calculate the total power carried by surface-wave fields the surface-wave contribution of equation (13) is evaluated by the residue theorem in a similar manner to equation (33) and the surface-wave field inside the rod is given by

$$H_{z1} = -4\,\Sigma\,\Sigma\, T_M(\beta_z, \beta_y)\,(D'_z\, D'_y)^{-1}\cos(\beta_z x)\,.$$

$$\times \cos(\beta_y y)\exp(-j\beta_z z), \qquad (45)$$

The total power carried by the individual surface-wave modes in all the five regions 1, 2, 3, 4, 5 is

$$P_s = \tfrac{1}{2}\{ \int_{-a/2}^{a/2}\int_{-b/2}^{b/2} E_{y1} H_{x1}^* \,dxdy + \int_{-b/2}^{b/2} dy \,(\int_{-\infty}^{-a/2} E_{y4} H_{x4}^* \,dx$$
$$+ \int_{a/2}^{\infty} E_{y2} H_{x2}^* \,dx) + \int_{-a/2}^{a/2} dx \,(\int_{-\infty}^{-b/2} E_{y5} H_{y5}^* \,dy$$
$$+ \int_{b/2}^{\infty} E_{y3} H_{x3}^* \,dy)\} \tag{46}$$

where the asterisk denotes the complex conjugate. E_y is derived from H_z using equation (5). H_{z4} and H_{z5} are obtained from H_{z2} and H_{z3} replacing α_x and α_y by $-\alpha_x$ and $-\alpha_y$ respectively. Only surface-wave contributions of H_z are taken in the above integrals. Integral in equation (46) can be readily evaluated. Surface-wave modes are orthogonal to each other. The total power carried by all modes is the sum of powers carried by each mode. Surface-wave modes are also orthogonal to radiation modes.

Total power radiated from the junction is

$$P_r = \tfrac{1}{2}\,\mathrm{Re} \int_{\theta=0}^{\pi/2}\int_{0}^{2\pi} (\vec{E} \times \vec{H}) \cdot \vec{e}_r\, r^2 \sin\theta \, d\theta \, d\phi \tag{47}$$

where $\vec{e}_r$ is the unit vector in the r-direction and θ and ϕ are the elevation and azimuthal angles in spherical polar co-ordinates. Components of $\vec{E}$ and $\vec{H}$ are given by equations (5), (41) and (42). This integral has been evaluated numerically. Instead of evaluating the double integral the values of the integral are evaluated at $\phi = 0°$ and $\phi = 90°$. Denoting the value of the integral by P_0 and P_{90} for $\phi = 0°$ and $\phi = 90°$ respectively all write

$$P_{0°} = \pi Z_0 \int^{\pi/2} |H_{z0}|^2 r^2 \sin\theta \sec^2\theta \, d\theta \tag{48}$$

$$P_{90°} = \pi Z_0 \int_{0}^{\pi/2} |H_{z90°}|^2 r^2 \sin\theta \, d\theta \tag{49}$$

where

$$Z_0 = (\mu_0/\varepsilon_0)^{1/2} \tag{50}$$

$H_{z0°}$ and $H_{z90°}$ are the total far-fields and are evaluated from equations (41) and (42) by putting $\phi = 0°$ (*i.e.*, $q = 0$) and $\phi = 90°$ (*i.e.*, $p = 0$) respectively. Total power radiated is[8]

$$P_r \simeq \tfrac{1}{2}(P_0 + P_{90}). \tag{51}$$

Launching efficiency is

$$\eta_s\,(\%) = 100\, P_s (P_s + P_r)^{-1} \tag{52}$$

has been calculated for several rectangular dielectric rods of different dimensions and compared with the measured values in Table I.

3. Experimental procedure

The experimental determination of launching efficiency involves the measurement of the scattering parameters of the composite structure, *i.e.*, the mode transducer and the dielectric rod following Deschamp's method[9].

(i) *Scattering matrix of the composite structure*

The experimental set-up is shown in Fig. 3. The complex reflection coefficients have been measured with the aid of a slotted section for eight different lengths 'l' of the dielectric rod. These lengths are taken in pairs $\beta_g l_1$, $\beta_g l_1 + \pi/2$ to $\beta_g l_4$, $\beta_g l_4 + \pi/2$ (β_g = phase constant of the particular mode in the dielectric rod). These four pairs of different lengths are distributed over half the guided wavelength ($= 2\pi\beta_g^{-1}$). The points are plotted on a polar chart and a circle is drawn through them. The iconocentre S_{11} is found out from the geometrical construction (Fig. 4). The method of finding out the elements of $[S]$ has been described in the literature[10] and will not be elaborated here but we shall consider the case when the modal attenuation of the dielectric rod cannot be neglected.

If α nepers/cm is the attenuation constant of the mode of the reflection coefficient at the plane BB (Fig. 3) is given by

$$\rho_L = \exp(-2\alpha l) \exp j(\phi_L - 2\beta_g l) \tag{53}$$

where ϕ_L is the phase of the reflection of the load terminating the dielectric rod (*i.e.*, the shorting plate). As the length 'l' is reduced the locus of ρ_L will spiral outward. When α is not very large the points still lie approximately on a circle because they are

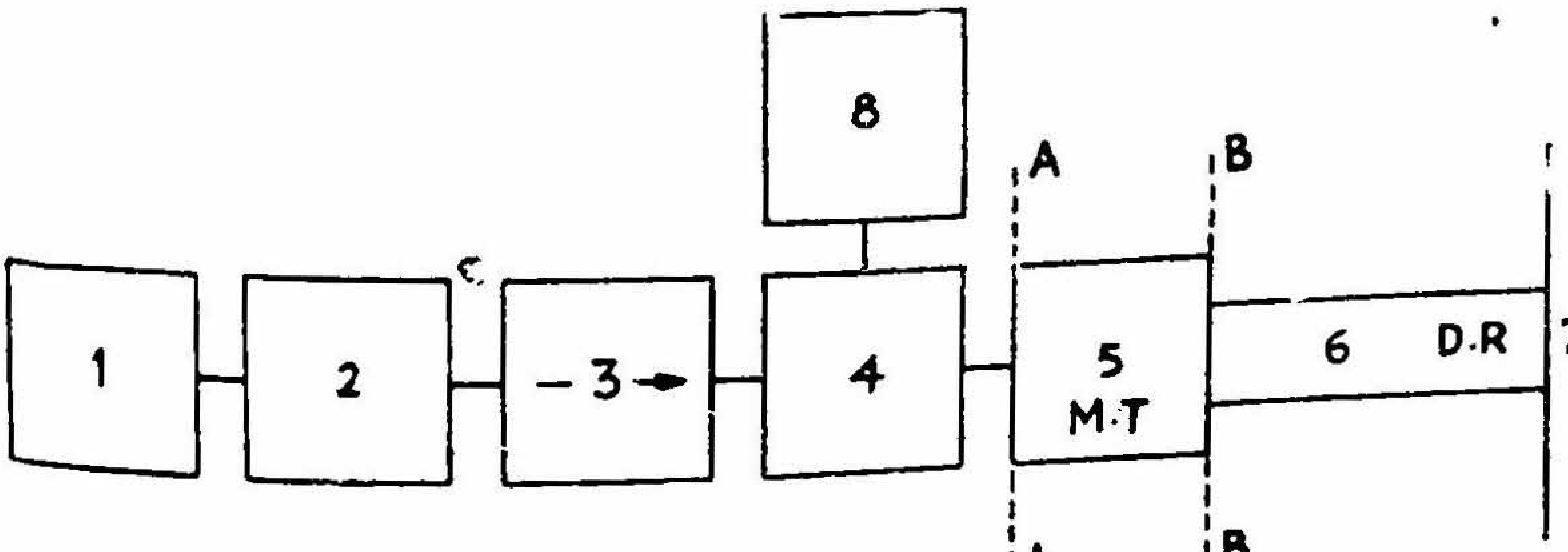

FIG. 3. Experimental set-up for scattering parameter measurements.
(1) Power supply and squarewave modulator, (2) Klystron 723A/B, (3) Isolator, (4) Slotted line (P.R.D.), (5) Mode transducer, (6) Dielectric rod, (7) Shorting plate, (8) V.S.W.R. meter (P.R.D.).

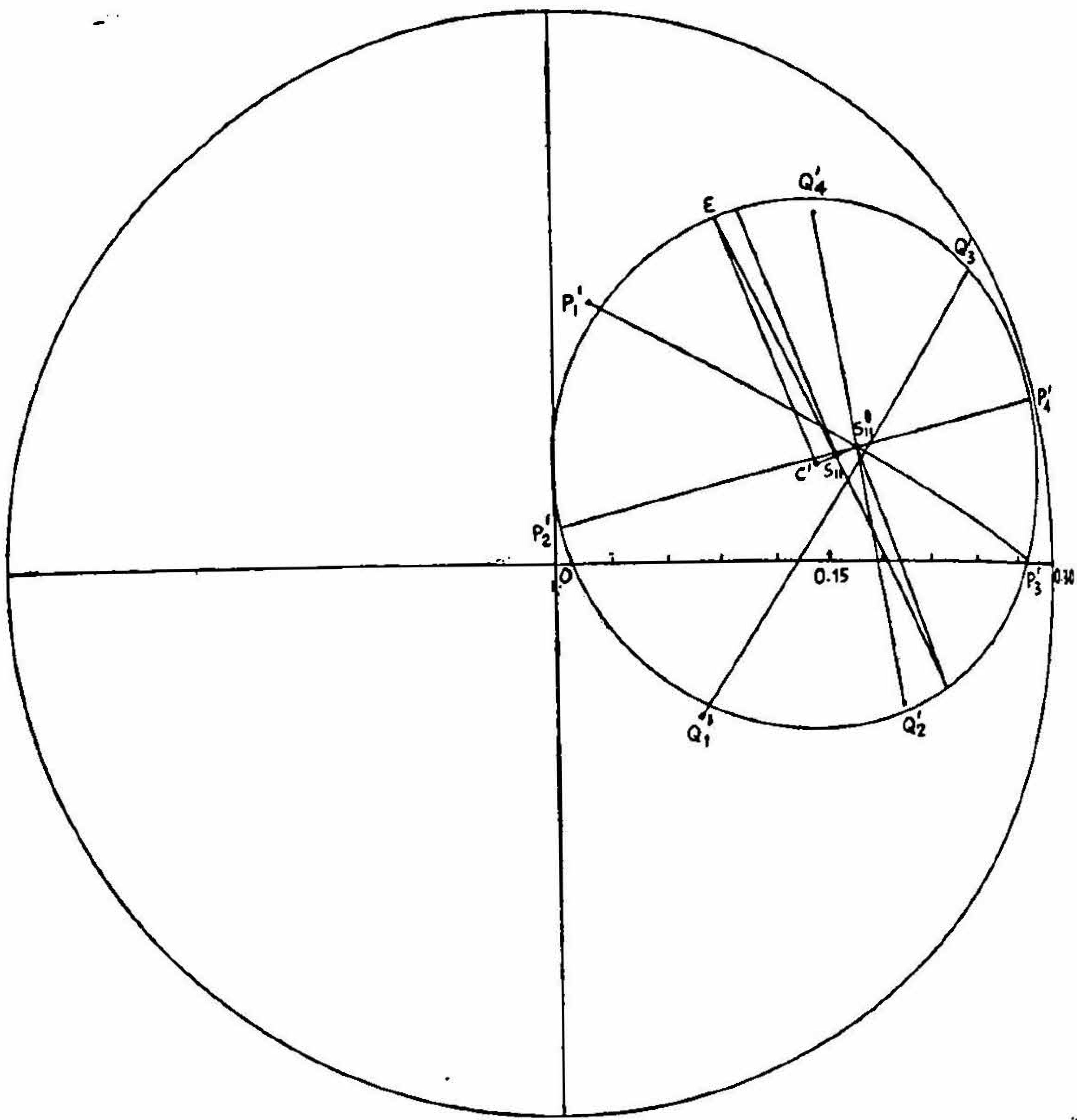

FIG. 4. Circle diagram leading to the evaluation of the scattering matrix [S] of the composite Structure $a = 0\cdot 895\ \lambda_0$, $b = 0\cdot 398\ \lambda_0$, $\lambda_0 = 3\cdot 2$ cm.

distributed over only half the guided wavelength of the rod ($\lambda_g \sim 2\cdot 5$ cms.). Hence the procedure described in reference 10 still applies if it is assumed that the dielectric rod is terminated in a load of reflection coefficient $\rho \exp j\,\phi_L$. Hence [eqn. 5, Ref. 10]

$$r = \frac{|S_{12}|^2\,|\rho|}{1 - |\rho|^2\,|S_{22}|^2} \tag{54}$$

$$|S_{22}| = \frac{S_{11}\,C'}{r\,|\rho|} \tag{55}$$

$$|S_{12}|^2 = \frac{S_{11}\,E^2}{r\,|\rho|} \tag{56}$$

where

$$\rho = \exp(-2\alpha l). \tag{57}$$

If the experiment is repeated for two widely different lengths l and l' of the rod, two different circles will be obtained because the load reflection coefficients will be different due to the attenuation of the rod.

If r, r', S_{11} E, $S_{11}E'$ are the corresponding values read from the two circle diagrams we write

$$|S_{12}|^2 = \frac{S_{11}E^2}{r\,|\rho|} \tag{58}$$

$$|S_{12}|^2 = \frac{S_{11}E'^2}{r\,|\rho'|} \tag{59}$$

where

$$\rho = \exp(-2\,\alpha l) \tag{60}$$

$$\rho' = \exp(-2\,\alpha l'). \tag{61}$$

Hence

$$e^{-2\alpha(l-l')} = \frac{r'\,S_{11}\,E^2}{r\,S_{11}\,E'^2} \tag{62}$$

or

$$\alpha = \frac{1}{2(l-l)}\, ln\left[\frac{r\,S_{11}\,E'^2}{r'\,S_{11}\,E^2}\right]. \tag{63}$$

Once α is determined from equation (63), the elements of $[S]$ can be found out from equations (55) and (56). S_{11} can be directly read from either of the circle diagrams OS_{11}.

(ii) *Scattering matrix of the mode transducer*

The scattering parameters measured in the above section represent the junction (plane AA in Fig. 3) between the slotted section and the composite structure. To find out the elements of the scattering matrix of the junction between the mode transducer (MT in Fig. 1) and the dielectric rod (DR in Fig. 1) the scattering matrix of the mode transducer has to be determined. This has been done by replacing the dielectric rod with a metal waveguide with a variable short. The cross-sectional dimension of the metal waveguide is identical to that of the mode transducer. By varying the position of the shorting plate the complex reflection coefficients are measured and from the circle diagram the elements of $[M]$ the scattering matrix of the mode transducer are found to be

$$M_{11} = 0{\cdot}25 < 1{\cdot}92 \text{ radian}$$

$$M_{22}' = 0 \cdot 32 < 2 \cdot 46 \text{ radian}$$

$$M_{21} = M_{12} = 0 \cdot 83 < 0 \cdot 69 \text{ radian.}$$

If $[N]$ represents the elements of the scattering matrix of the mode transducer and the dielectric rod junction we have[11]

$$\begin{aligned} N_{11} &= (S_{11} - M_{11})(M_{21} M_{12} - M_{22} M_{11} + S_{11} M_{11})^{-1} \\ N_{12} &= S_{12}(1 - N_{11} M_{12})(M_{12})^{-1} \\ N_{21} &= S_{21}(1 - M_{22} N_{11})(M_{21})^{-1} \\ N_{22} &= S_{22} - N_{21} M_{22}(1 - N_{11} M_{22})^{-1}. \end{aligned} \quad (65)$$

(iii) *Launching efficiency*

The launching efficiency η_s of the mode transducer can be determined from the elements of $[N]$ as follows:

$$\eta_s (\%) = 100 \,|\, N_{12} \,|^2 / (1 - |\, N_{11} \,|^2)^{-1}. \quad (66)$$

Both the theoretical and the experimental values of the launching efficiencies, the elements of $[N]$ and attenuation constant α of the rods are given in Table I as functions of rod cross-sectional dimensions. For all the rods the mode transducer has the dimension of RG51U. The calculated values of η_s are given in Table I.

Table I

Comparision of the theoretical and the experimental values of launching efficiencies at $\lambda_0 = 3 \cdot 2$ cms

$\frac{a}{\lambda_0}$	$\frac{b}{\lambda_0}$	α db/m	$\lvert N_{11} \rvert$	$\lvert N_{22} \rvert$	η_s% Theory	η_s% Experiment
0·635	0·545	12·5	0·43	0·32	77·64	81·1
0·795	0·795	12·5	0·46	0·24	77·23	88·0
0·895	0·398	10·9	0·34	0·26	78·81	83·5

4. Conclusions

A few points are worth noting in Table I. The high values of $|N_{11}|$ indicate high reflection loss from the junction of the mode transducer and the dielectric rod and hence it is realised that the simple form of tapering the dielectric material inside the metal waveguide is not adequate for reducing the reflection loss.

The difference in the values of $|N_{11}|$ and $|N_{22}|$ indicates that the junction between the mode transducer and the dielectric rod is not lossless. This is indeed true because there will always be radiation from the junction. In fact the junction can be treated as a three-port one, the third port corresponding to the radiation from the junction. The experimental results quoted in Table I have been obtained by considering a two-port measurement procedure. The radiation from the junction is completely lost in free-space and following the method for a three-port junction[12] and assuming that there is no reflection from the termination of the third port the above procedure will still yield the correct values of the elements of $[N]$ as given in the table.

The discrepancy in the theoretical and the measured values of η_s is expected due to two reasons mainly, *viz.*, the approximate method of finding out the radiated power [eqn. 51] and ignoring the effect of the tapered portion of the rod outside the mode transducer.

5. Acknowledgement

The authors take this opportunity to thank Prof. S. Dhawan, Director of Indian Institute of Science, for providing all the facilities for the above work. They also wish to thank Prof. S. K. Chatterjee, Hon. Retired Professor, Indian Institute of Science, for helpful discussions.

Appendix

Evaluation of the integrals by stationary phase method

From equation (39) we write

$$I = -\frac{2j}{4\pi^2 D'} I' \tag{A.1}$$

where

$$I' = \int_{-\infty}^{\infty} \int_{\Gamma_1} T_M(k_x, \beta_y) \left[\frac{\sin(Rb/2)}{R} + \frac{\sin(Sb/2)}{S}\right] \times (1+\rho_z)(D_z)^{-1} \exp j\,[(p-k_z)\,a/2 - px - k_y y - k_z z] \times dk_x\, dk_y \tag{A.2}$$

Changing the integration variable k_x to p we write

$$I' = \int_{-\infty}^{\infty} \int_{-\infty}^{\infty} \frac{p \exp[\,j(p-k_z)\,a/2]}{k_z D_z} T_M(k_x, \beta_y) \left[\frac{\sin(Rb/2)}{R} + \frac{\sin(Sb/2)}{S}\right] (1+\rho_z) \exp[-j(px + k_y y + k_z z)]\, dp\, dk_y \tag{A.3}$$

where k_z is related to p given by equation (16).

Let

$$I' = \int_{-\infty}^{\infty} \int_{-\infty}^{\infty} g(p, k_y) \exp[-j(px + k_y y + k_z z)]\, dp\, dk_y \tag{A.4}$$

where

$$g(p, k_y) = \frac{p \exp[j(p - k_z)\, a/2]}{k_z D_z} T_M(k_z, \beta_y)$$

$$\times \left[\frac{\sin(Rb/2)}{R} + \frac{\sin(Sb/2)}{S}\right](1 + \rho_z). \tag{A.5}$$

In terms of polar co-ordinates we write

$$\begin{aligned} p &= k_0 \sin\theta \cos\phi \\ k_y &= k_0 \sin\theta \sin\phi \\ k_z &= k_0 \cos\theta \\ x &= r \sin\theta_0 \cos\phi_0 \\ y &= r \sin\theta_0 \sin\phi_0 \\ z &= r \cos\theta_0 \end{aligned} \tag{A.6}$$

where (θ, ϕ) is the direction of the ray and (r, θ_0, ϕ_0) is the observation point. Thus

$$\begin{aligned} px + k_y y + k_z z &= k_0 r [\sin\theta \sin\theta_0 \cos(\phi - \phi_0) + \cos\theta \cos\theta_0] \\ &= k_0 r f(\theta, \phi). \end{aligned} \tag{A.7}$$

Changing the integration variable to θ, ϕ we obtain

$$I' = k_0^2 \int\int g(\theta, \phi) \exp[-jk_0 r f(\theta, \phi)] \sin\theta \cos\theta\, d\theta\, d\phi. \tag{A.8}$$

The points of stationary phase are determined by

$$\frac{\partial f(\theta, \phi)}{\partial\theta} = 0 \tag{A.9}$$

$$\frac{\partial f(\theta, \phi)}{\partial\phi} = 0 \tag{A.10}$$

which yield

$$\theta = \theta_0 \tag{A.11}$$

$$\phi = \phi_0. \tag{A.12}$$

Hence the value of the integral is given by [Ref. 13 pp. 753–754]

$$I' = k_0^2 g(\theta_0, \phi_0) \sin\theta_0 \cos\theta_0 \frac{\exp[-jk_0 r f(\theta_0, \phi_0)]}{k_0 r} \frac{2\pi j}{(\alpha\delta - \gamma^2)^{1/2}} \tag{A.13}$$

where

$$\alpha = \left.\frac{\partial^2 f}{\partial \theta^2}\right|_{\substack{\theta=\theta_0\\ \phi=\phi_0}} \tag{A.14}$$

$$\delta = \left.\frac{\partial^2 f}{\partial \phi^2}\right|_{\substack{\theta=\theta_0\\ \phi=\phi_0}} \tag{A.15}$$

$$\gamma = \left.\frac{\partial^2 f}{\partial \theta\, \partial \phi}\right|_{\substack{\theta=\theta_0\\ \phi=\phi_0}} . \tag{A.16}$$

Evaluating α, δ, from equations (A.14) to (A.16) we obtain

$$\begin{aligned} \alpha &= -1 \\ \delta &= -\sin^2\theta_0 \\ r &= 0 \end{aligned} \tag{A.17}$$

Hence

$$I' = \frac{2\pi j}{r} k_{z0}\, g(\theta_0, \phi_0) \exp(-jk_0 r) \tag{A.18}$$

where

$$k_{z0} = k_0 \cos\theta_0 . \tag{A.19}$$

Inserting $g(\theta_0, \phi_0)$ from equation (A.5) we obtain

$$I_1 = \frac{2\pi j k_z^0}{4\pi^2 r}\left(-\frac{2j}{D'_\gamma}\right)\frac{p \exp[j(p-k_z)a/2]}{k_z D_z} T_M(k_x, \beta_y)$$

$$\times (1+\rho_z)\left[\frac{\sin(Rb/2)}{R} + \frac{\sin(Sb/2)}{S}\right]\exp(-jk_0 r) . \tag{A.20}$$

References

1. BARLOW, H. M. AND BROWN, J. — *Radio Surface Waves*, 1962, Ch. 10, Clarendon.
2. COLLIN, R. E. AND ZUCKER, F. J. — *Antenna Theory*, 1969, pt. 2, Ch. 21, McGraw-Hill.
3. WENGER, N. C. — The launching of surface waves on an axially-cylindrical reactive surface, *I.E.E.E. Trans.*, AP-13, 1965, 126–134.
4. BOOKER, H. C. AND CLEMMOW, P. C. — The concept of an angular spectrum of plane waves and its relation to polar diagram, *Proc. I.E.E.*, 1950, 97, 11–17, (Pt. III).
5. BLAKEY, J. R. — Calculation of dielectric-aerial radiation patterns, *El. Lett.*, 1968, pp. 46–47.

6. MARCATILI, E. A. J. Dielectric rectangular waveguide and directional co integrated optics, *B.S.T.J.*, 1969, **48**, 2071–2102.

7. SMIRNOV, V. I. *A Course of Higher Mathematics*, 1964, Pt. II, pp Pergamon Press.

8. SILVER, S. *Microwave Antenna Theory and Design*, 1949, Ch. 15 581, McGraw-Hill.

9. DESCHAMP, G. A. Determination of reflection coefficient and insertionloss guide junction, *J. Appl. Phys.*, 1953, **28**, 1046–1050.

10. STORER, J. E., SHEINGOLD, L. S. AND STEIN, S. A simple graphical analysis of a two-port junction, *P* 1953, **41**, 1004–1013.

11. KERNS, D. M. AND BEATTY, R. W. *Basic Theory of Waveguide Junctions and Introductory Network Analysis*, 1967, pp. 72–76, Pergamon Press.

12. STEIN, S. Graphical analysis of measurements on multiport junctions, *Proc. I.R.E.*, 1954, **42**, 599.

13. BORN, M. AND WOLF, E. *Principles of Optics*, 1965, Pergamon Press.